[CANCER RESEARCH 64, 5587–5591, August 15, 2004]

Cyclooxygenase-1 Deletion Enhances Apoptosis but Does Not Protect Against Ultraviolet Light-Induced Tumors

Alice P. Pentland,[1] Glynis Scott,[1] JoAnne VanBuskirk,[1] Carol Tanck,[1] Gina LaRossa,[1] and Sabine Brouxhon[2]

Departments of [1]Dermatology and [2]Emergency Medicine, University of Rochester Medical Center, Rochester, New York

ABSTRACT

Inhibition or deletion of cyclooxygenase (COX)-2 has been demonstrated to protect against squamous cell cancer in many studies. Although much effort has focused on COX-2 inhibition, recent work indicates that COX-1 deletion may be nearly as protective. In this study, we used SKH-1 hairless mice in which COX-1 was selectively deleted to examine the role of COX-1 in photocarcinogenesis. After UV exposure, 40–60% less prostaglandin E_2 was detected in COX-$1^{-/-}$ animals compared with wild-type (WT) controls. A 4-fold induction of keratinocyte apoptosis was observed in knockouts relative to WT animals, as documented by terminal deoxynucleotidyl transferase (TdT)-mediated dUTP nick end labeling and caspase-3 staining. Proliferation was not significantly different in COX-$1^{+/+}$, COX-$1^{+/-}$, and COX-$1^{-/-}$ animals. When susceptibility to UV-induced tumor formation was studied, tumor number, average tumor size, and time of tumor onset in COX-$1^{-/-}$ animals were identical to WT controls. Thus, enhanced apoptosis did not alter UV-induced skin carcinogenesis, suggesting other effects are key to nonsteroidal anti-inflammatory drug chemoprevention. These results contrast sharply with data obtained using the classic 7,12-dimethylbenz(*a*)anthracene/12-*O*-tetradecanoylphorbol-13-acetate cancer model in which a prominent protective effect of COX-$1^{-/-}$ is present. The lack of protection observed here confirms cancer mechanisms are distinct in UV- and tumor promotor-induced cancer models and indicates that chemoprevention strategies must specifically address cancer causes to be effective.

INTRODUCTION

Exposure of skin to UV light is the major cause of skin cancer (1, 2). Skin cancer is on the rise, with ~1 million Americans developing a nonmelanoma skin cancer each year, and about half of all white persons expected to develop one in their lifetime. The prognosis is poor in recurrent squamous cell carcinoma, because the cure rate is only ~50%. In addition, the cost of treating nonmelanoma skin cancer exceeds $500 million per year. It is clear that effective skin cancer chemoprevention could have a large health impact (3, 4).

UV exposure increases prostaglandin (PG) production in the skin (5). Prostaglandin E_2 (PGE_2) is the predominant PG formed in human epidermis (6, 7), and it is a powerful regulator of keratinocyte proliferation and differentiation (8). Synthesis of PGs occurs through the action of cyclooxygenase (COX) enzymes that convert arachidonic acid into PGs. Two major isoforms of COX exist, COX-1 and COX-2 (9). COX-1 is constitutively expressed, whereas COX-2 is induced by UV exposure. COX-2 expression is also induced in malignancies of the gut and prostate as well as skin (10–14). *In vivo* COX-2 inhibition by administration of selective COX-2 inhibitors has been demonstrated to inhibit mouse tumorigenesis in many studies, including UV irradiation and 7,12-dimethylbenz(*a*)anthracene (DMBA)/12-*O*-tetradecanoylphorbol-13-acetate murine carcinogenesis models (15–19). In studies of tumor promotion in mice with selective deletions of COX-1 or COX-2, deletion of either isoform resulted in protection in intestinal (20) as well as skin tumor models. When apoptosis or proliferation are examined in these studies, apoptosis was found to be increased significantly by deletion of either COX isoform, whereas 12-*O*-tetradecanoylphorbol-13-acetate-stimulated proliferation was found to be decreased (21). Similar results were obtained when a selective COX-2 inhibitor is used (22). Most work indicates that effects on apoptosis and proliferation are both important for protection against tumor formation. Apoptosis is thought to be crucial for removing cells with mutations, whereas proliferation dramatically increases the number of clones containing mutations, which then only need a second mutation to complete their cancerous transformation. Work generally points to an important role for apoptosis and proliferation in the cancer chemoprevention provided by selective COX inhibitors (14, 16).

In this study, we used SKH hairless mice with a selective deletion of COX-1 to examine its role in epidermal responses after UV irradiation. Our data show that absence of COX-1 increases substantially apoptosis 4-fold in irradiated animals, although producing little effect on proliferation. Unlike other studies in which COX-1 deficiency protected animals against tumorigenesis (20, 21), UV-irradiated COX-1-deficient animals were not protected. This data suggests that other mechanisms have a greater impact on UV-induced tumor formation than apoptotic responses. It additionally indicates that classic models using DMBA initiation followed by 12-*O*-tetradecanoylphorbol-13-acetate tumor promotion may not be useful for predicting efficacy of chemopreventive agents targeted against UV light-induced tumors. Most importantly, this data argues that chemoprevention strategies must consider specifically the etiology of cancers they are intended to prevent.

MATERIALS AND METHODS

Animals. COX-$1^{-/-}$ animals were the kind gift of Dr. Don Young (University of Rochester, Rochester, NY) and were originally bred by Dr. Robert Langenbach (Experimental Carcinogenesis Laboratory, Research Triangle Park, NC; Ref. 23). Animals were initially in a C57bl6/SV129 background. They were backcrossed seven generations into SKH-1 mice obtained from Charles River Laboratories (Wilmington, MA) to create albino hairless mice lacking COX-1. Outbred SKH-1 mice are the standard strain used for photocarcinogenesis work (24). The SKH-1 hairless mouse has a defect in hair catagen regulation (25, 26). In all other respects, the skin of this mouse is considered normal and is not immunocompromised (22, 26). When 5 representative animals were checked by genetic typing using a C57Bl marker panel of 97 markers, 73% of the loci tested were homozygous among the animals, and another 17% were heterozygous. Overall, 27% of the loci were the same as the C57Bl strain. Six- to 7-week-old mice weighing between 25 and 30 g were used. The mice were housed 5/cage under constant humidity and temperature with 12-h light/dark cycles. They were allowed access to water and standard mouse feed *ad libitum* and were monitored daily. All of the experimental procedures received approval by the Institutional Laboratory Animal Care and Use Committee of the University of Rochester Medical Center.

UV Irradiation. The dorsal skin of wild-type (WT), COX-$1^{+/-}$, and COX-$1^{-/-}$ mice was exposed to UV irradiation in groups of 2 or 3, using a bank of 4 UVA Sun 340 sunlamps (Q-Panel Lab Products, Cleveland, OH). UVA Sun 340 sunlamps emit UV between 295 and 390 nm, which include both UVA and UVB wavelengths. Lamp emission closely resembles the UV spectrum of sunshine through the mid-UVA range (22). Lamp output was

Received 3/24/04; revised 4/27/04; accepted 6/22/04.

Grant support: Grants RO1-AR46828 and NIH-AR07472.

The costs of publication of this article were defrayed in part by the payment of page charges. This article must therefore be hereby marked *advertisement* in accordance with 18 U.S.C. Section 1734 solely to indicate this fact.

Requests for reprints: Alice P. Pentland, Department of Dermatology, University of Rochester, 601 Elmwood Avenue, Box 697, Rochester, NY 14642. Phone: (585) 275-1998; Fax: (585) 273-1346; E-mail: Alice_Pentland@urmc.rochester.edu.

measured by an IL1700 light meter (International Light, Newburyport, MA), using a SED 240 probe for measurement of the UVB portion of the lamp spectrum. The SED 240 probe detects wavelengths from 255 to 320 nm. Doses stated represent this portion of the lamp output only. The mice were exposed to UV at a distance of 15 inches. Heat produced by the lamp was negligible under these conditions. The total dose was calculated using the measured value and the length of exposure. Animals were irradiated acutely with 180 mJ/cm^2 UVB, a dose that is environmentally relevant, as it is equivalent to 60 min of noonday summer sun in Rochester, NY. Animals were exposed to the lamps 3 times/week for 15 weeks. In chronically irradiated animals, the dose was increased 10%/week to the maximum length exposure of 300 min. The cumulative UVB dose was 12 J/cm^2. The UVA cumulative dose was 658 J/cm^2. Twelve animals per group completed the irradiation protocol.

Morphological Studies and Immunohistochemical Analysis. After sacrifice, mouse dorsal skin was collected, fixed in 10% neutral buffered formalin, routinely processed, and embedded in paraffin. Paraffin sections (5 μm) stained with H&E were used for histological analysis of UV-induced alterations in morphology and diagnosis of mouse tumors by Dr. Scott. Measurements of epidermal thickness were made using these sections. For the immunolocalization of COX-1, COX-2, and caspase-3, a protocol described by Brouxhon *et al.* (27) was used. Tissue samples were fixed in 10% formalin overnight, placed in graded alcohol solutions, paraffin-embedded, and then cut into 5-μM sections. Samples were subsequently deparaffinized, blocked in 4% normal goat serum, and then incubated overnight in either anti-COX-2 (Cayman Chemical, Ann Arbor, MI), anti-COX-1 (Cayman Chemical), or anti-caspase-3 (Cell Signaling, Beverly, MA) polyclonal antibodies plus 0.4% Triton-X, 1% BSA, and 4% normal goat serum at 4°C. The next day, slides were incubated with goat antirabbit IgG antibody conjugated with biotin (Vector Elite Kit; Vector Laboratories, Burlingame, CA) for 90 min, rinsed with PBS, incubated for 60 min with an avidin-biotin-peroxidase complex (Vector Laboratories), and developed in an acetate-imidazole buffer containing 0.05% 3,3-diaminobenzidine (Sigma Chemical Co., St. Louis, MO) and 0.01% hydrogen peroxide with nickel enhancement. Control sections for antibody specificity were processed simultaneously in the absence of primary antibody or with appropriate isotype controls. Assessment of intensity of caspase staining was graded 0 to 3+ by four reviewers who were blinded to the identity of the tested slides.

Measurement of PGs in Mouse Epidermis. After sacrifice, mouse dorsal skin was snap frozen, and the epidermis curetted directly into ice-cold methanol. Efficacy of curettage as a method for removing epidermis only was documented by histology. Samples were spiked with thromboxane B_2 (Cayman Chemical) for estimation of extraction efficiency, buffered with 0.1 M NaH_2PO_4 (pH 4.0), and then individually loaded onto C-18 solid-phase extraction cartridges (Waters, Milford, MA) preconditioned with ethanol and H_2O (pH 4). After washing with H_2O (pH 4.0) and hexane, samples were eluted by gravity with ethyl acetate/1% methanol. The eluant was dried under nitrogen and reconstituted with EIA Buffer (Cayman Chemical). The PGE_2 and $PGF_{2\alpha}$ levels in the samples were determined using PGE_2 EIA kits according to the manufacturer's instructions (Cayman Chemical). Similarly, thromboxane B_2 levels were determined with a thromboxane B_2 EIA kit (Cayman Chemical), and extraction efficiencies were calculated from the results.

Keratinocyte Proliferation. Keratinocyte proliferation in mouse epidermis was measured using immunohistochemical detection of bromodeoxyuridine (BrdUrd). Mice were injected i.p. with 0.3 ml of a 20 mM solution of BrdUrd (Boehringer Mannheim, Mannheim, Germany) 3 h before sacrifice. BrdU was detected with the BrdU staining kit (Zymed Laboratories Inc., San Francisco, CA) according to the manufacturer's recommendations and was visualized with the VIP chromagen (Vector Laboratories). The sections were counterstained briefly with blue/methyl green (Rowley Biochemical Institute, Danvers, MA). A section of small intestine was included from each mouse as a positive control for BrdUrd incorporation. Quantitation of BrdUrd proliferation was blinded and expressed as the ratio of BrdUrd-positive nuclei to 10,000 μm^2. A minimum of 6–8 fields was evaluated per section. BrdUrd-labeled cells in normal or tumor tissue were tabulated separately. Cells within follicular cysts were not counted (22).

Keratinocyte Apoptosis. Apoptosis was evaluated on skin sections by the terminal deoxynucleotidyl transferase (TdT)-mediated dUTP nick end labeling (TUNEL) method (22). TUNEL staining was achieved by labeling fragmented DNA with fluorescein-labeled dUTP and terminal deoxynucleotidyl transferase, using the commercially available Apoptosis Detection System (Promega, Madison, WI). The fragmented DNA was visualized by fluorescent microscopy.

Statistical Analyses. For experiments evaluating the number of tumors in irradiated animals, a Kruskal-Wallis rank test was performed on each group (28). Other statistical analyses were performed by computer assisted two-tailed ANOVA to compare between group means. The analyses were performed on the raw data values (parametric analysis) using the least significant differences means comparison procedure. The comparisons to the control groups were assessed using one-tailed tests. A P of 0.05 ($P < 0.05$) was considered statistically significant. Data are expressed as mean ± SE.

RESULTS

Characterization of UV-Induced Skin Injury. Groups of SKH-1 WT, COX-1$^{+/-}$, and COX-1$^{-/-}$ mice were exposed to 180 mJ/cm^2 of light, then examined 24 and 72 h after exposure. This dose of light is 30% greater than the minimal dose required to produce an increase in the thickness of mouse skin, as measured by micrometer histologically. On routine histological examination, typical findings of UV irradiation were observed, including a modest increase in epidermal thickness (22). The response to irradiation was the same among the different genotypes (data not shown).

When skin sections from animals were examined after 15 weeks of chronic UV exposure, pronounced hyperplasia of the epidermis was evident. Little or no inflammatory infiltrate was present. Measurement of epidermal thickness showed a 5-fold increase in skin of irradiated animals compared with unirradiated controls (Table 1). In chronically UV-exposed animals, an increase in the spinous layer, a pronounced granular layer, and a thickened keratin layer were present. Little difference was observed in the morphology of the epidermis between the genotypes.

Characterization of COX Isoform Expression and PG Synthesis After UV-Induced Skin Injury. Acute UV irradiation induced COX-2 expression 24 h after exposure in WT and knockout mice. Induction of COX-2 expression was also evident in chronically irradiated animals at the 15- and 30-week time points of the protocol. In COX-1$^{-/-}$ animals, COX-2 was also detected in animals that were not irradiated when compared with WT controls. However, no excess induction of COX-2 by UV exposure occurred in animals lacking COX-1. As expected, COX-1 staining revealed no immunoreactive protein in COX-1$^{-/-}$ animals (Fig. 1).

The quantity of PGE_2 and $PGF_{2\alpha}$ in epidermis at the time of sacrifice was also studied. PGE_2 was found to be present in the greatest quantity, and so its synthesis was followed as a measure of UV effects on PG synthesis. UV exposure significantly induced PGE_2 synthesis, as illustrated in Table 2. The epidermal PGE_2 content detected in COX-1$^{-/-}$ animals was only 60% of that observed in WT animals, and the quantity of PGE_2 observed in COX-1$^{+/-}$ animals was intermediate between WT and $^{-/-}$ animals.

Table 1 *Epidermal thickness remains unchanged with COX-1 gene disruption and chronic UV-irradiation*

	WT (mm thickness)	COX-1$^{+/-}$ (mm thickness)	COX-1$^{-/-}$ (mm thickness)
Control	24.6 ± 0.474	27.2 ± 0.47	32.9 ± 5.30
UV	117.8 ± 15.51	129.1 ± 18.3	115.1 ± 13.9

NOTE: Skin from Skh:hairless mice exposed to 15 weeks of chronic UV irradiation were assessed for epidermal thickness. UV irradiation produced a 5-fold increase in epidermal thickness compared to unirradiated controls (Tukey *post hoc* analysis). No significant difference in epidermal thickness was noted among COX-1$^{-/-}$, COX-1$^{+/-}$, or wild-type genotypes in either UV-irradiated or control groups. Results are expressed as mean ± SE (n = 4).

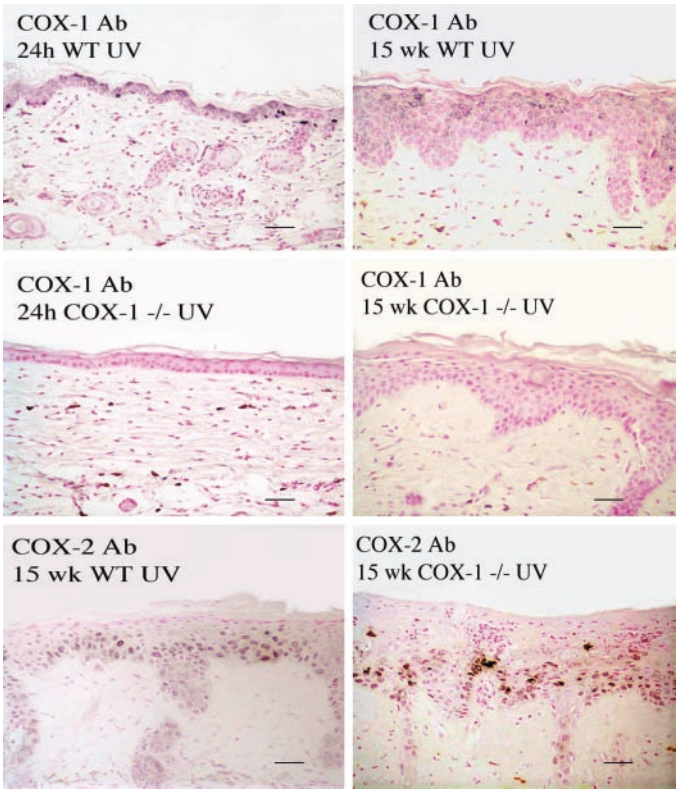

Fig. 1. Immunostaining of COX-1$^{-/-}$ mice. Staining for COX-1 and COX-2 are shown as described in "Materials and Methods." As expected, in COX-1 knockout animals, no immunoreactive material was present. *Scale bar,* 40 μm; hematoxylin counterstain.

Table 2 *Effects of COX-1 gene disruption on acute and chronic UV-induced PGE_2 levels in epidermis*

	PGE_2 (pg/mg)		
	COX-1$^{+/+}$	COX-1$^{+/-}$	COX-1$^{-/-}$
0 h	183 ± 22	197 ± 66	124 ± 20
24 h	393 ± 18	349 ± 14	243 ± 37
72 h	271 ± 46	212 ± 16	91 ± 9

NOTE: Using the solid-phase extraction method described in "Materials and Methods," epidermal curettings from mouse dorsal skin were assessed for PGE_2 levels by enzyme immunoassay. Data represent an acute (0–72 h) time course of UV-induced skin irradiation injury. PGE_2 is reduced significantly in COX-1$^{-/-}$ animals compared with controls at each time point. Data shown are mean ± SE; *P*s for $PGE_2 \leq 0.05$ (WT, $n = 4$; COX-1$^{+/-}$, $n = 4$; and COX-1$^{-/-}$, $n = 4$).

Loss of COX-1 Does Not Affect Proliferation but Does Increase Keratinocyte Apoptosis. Keratinocyte proliferation within the interfollicular epidermis of unirradiated animals was minimal at baseline in all three genotypes, with very small changes produced by the small doses of light used at the beginning of the photocarcinogenesis protocol. The effect of irradiation on keratinocyte proliferation was examined next (Fig. 2). Twenty-four h after the last UV exposure in the chronic irradiation protocol, (a cumulative UV dose of 12 J/cm^2) proliferation was increased 15-fold over unirradiated controls. This UV-mediated induction was statistically the same in all three genotypes, although a trend toward decreased proliferation in COX-1$^{-/-}$ mice was suggested compared with WT and COX-1$^{+/-}$ mice.

Exposure of the animals to UV in the small doses used for the acute protocol did not significantly induce the formation of apoptotic keratinocytes, classically known as sunburn cells, as measured by TUNEL analysis (Fig. 3). Very few TUNEL-positive cells were observed before UV exposure in each genotype. However, 24 h after the last UV irradiation of the 15-week irradiation protocol, a substantial increase in the number of TUNEL-positive cells was observed. Furthermore, a very strong effect of genotype was observed on apoptosis. UV-irradiated animals lacking COX-1 had 4-fold more TUNEL-positive cells than UV-irradiated WT animals. As was observed when PGE_2 was analyzed, an intermediate level of TUNEL staining was observed in heterozygous animals. To additionally confirm this alteration in apoptosis, immunohistochemistry was used to detect caspase 3 activation (Fig. 4). COX-1$^{-/-}$ animals had substantially more caspase staining than WT controls, confirming the studies using TUNEL staining.

Loss of COX-1 Does Not Affect UV-Induced Tumor Onset or Numbers. Because apoptosis was highly modulated by the presence of the COX-1 gene, the COX-1$^{-/-}$ animals presented the opportunity to study whether increased apoptosis occurring without significant changes in proliferation could reduce UV-induced tumor formation. Total tumor number and tumors per mouse were tracked over time (Fig. 5). No significant differences in the number of tumors, their time of onset, or tumor incidence per mouse was found. Histologic exam-

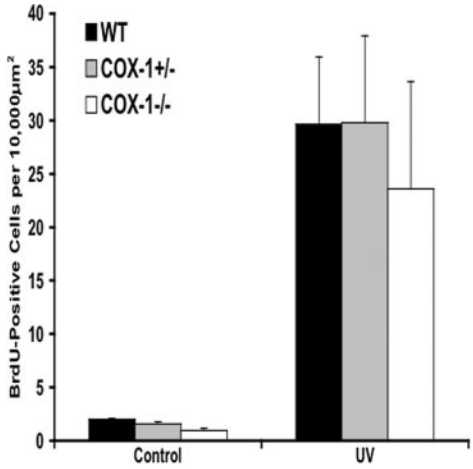

Fig. 2. COX-1 gene disruption does not affect keratinocyte proliferation in chronically irradiated animals. After 15 weeks of chronic UV exposure, BrdUrd uptake was measured in epidermis of Skh:hairless mice as described in "Materials and Methods." Data represent mean for WT control ($n = 6$), COX-1$^{+/-}$ ($n = 8$), and COX-1$^{-/-}$ ($n = 4$) mice. No significant differences were present using Tukey test. *Bars,* ±SE.

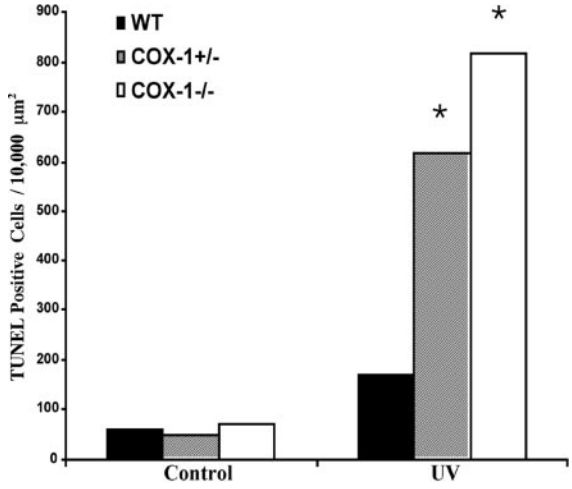

Fig. 3. UV irradiation markedly increases keratinocyte apoptosis in COX-1 knockout mice. A significantly higher number of TUNEL-positive apoptotic cells were detected in COX-1$^{-/-}$ *versus* WT controls. An intermediate number of apoptotic cells were present in the COX-1$^{+/-}$ genotype. Apoptosis was detected *in situ* using a TUNEL stain, as described in "Materials and Methods." WT controls, $n = 4$; COX-1$^{+/-}$, $n = 4$; and COX-1$^{-/-}$, $n = 4$. *, $P < 0.05$, Tukey test *versus* WT UV.

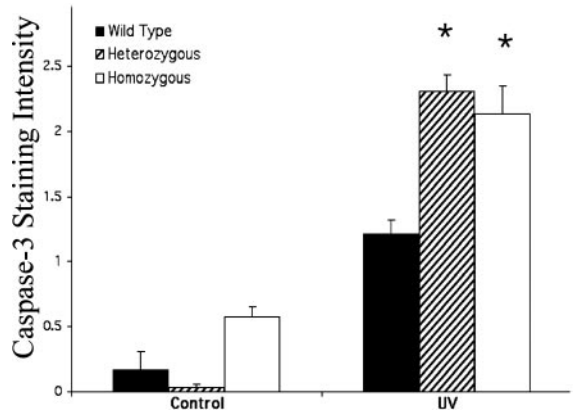

Fig. 4. COX-1 gene disruption enhances caspase-3 expression in the epidermis after chronic UV irradiation. Immunohistochemical staining revealed an ~4-fold induction of caspase-3 immunoreactivity in chronically irradiated COX-1$^{-/-}$ animals *versus* WT controls. Staining was most evident in the stratum granulosum as well as in the basal keratinocyte layer. WT controls, $n = 4$; COX-1$^{+/-}$, $n = 4$; and COX-1$^{-/-}$, $n = 4$. *, $P < 0.05$, Tukey test *versus* WT UV. *Bars*, ±SE

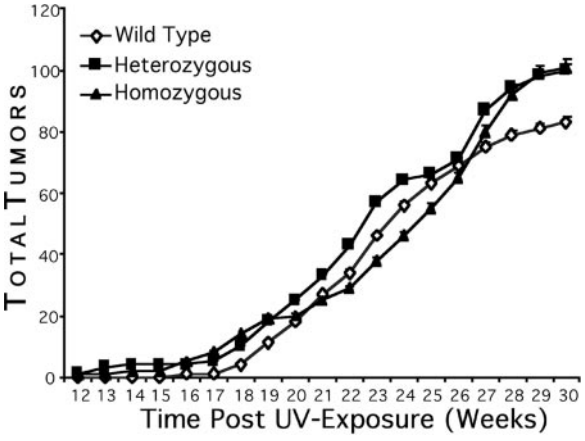

Fig. 5. UV-induced tumor numbers and time of onset are not affected by COX-1 gene disruption. Total tumors per mouse were counted weekly for 15 weeks after cessation of UV irradiation. In all of the cases, histologic diagnosis revealed squamous cell carcinoma with a similar histological grade that was independent of the genotype. Using a Kruskal-Wallis test, no significant differences were present among groups. WT controls, $n = 12$; COX-1$^{+/-}$, $n = 14$; and COX-1$^{-/-}$, $n = 13$. In all of the cases, histologic diagnosis revealed squamous cell carcinoma with a similar histological grade that was independent of the genotype. *Bars*, ±SE.

ination of tumors revealed squamous cell carcinoma in all of the cases. Precursor lesions, such as actinic keratosis-like lesions and Bowen's disease (squamous cell carcinoma *in situ*) were also apparent. There were no appreciable differences in the histological grade of the tumors based on genotype. At the end of the protocol, the average size of tumors present was calculated for each genotype. No differences were present (Table 3).

DISCUSSION

In this study, we demonstrated that deletion of COX-1 increases UV-induced apoptosis, without influencing proliferation in UV-irradiated SKH hairless mice. As expected, the absence of COX-1 reduced the quantity of PG present in knockout animal epidermis. Unexpectedly, the large change in apoptosis observed in COX-1$^{-/-}$ animals did not influence the number of tumors, their average final size, or the time when tumors appeared. These data are in sharp contrast to previous work examining the potential protective effects of COX-1$^{-/-}$ disruption on tumor development in other model systems. Using the *Min* mouse, which spontaneously develops intestinal polyps, Chulada *et al.* (20) found a 77% reduction in intestinal polyps in COX-1$^{-/-\ Min/+}$ mice compared with controls. Using a standard, DMBA/12-*O*-tetradecanoylphorbol-13-acetate chemical carcinogenesis model, Tiano *et al.* (21) found that COX-1 $^{-/-}$ knockout animals were substantially more resistant to a chemical carcinogenesis protocol. In these studies, COX-1 deletion reduced significantly the number of skin papillomas per mouse (nearly 50%) and significantly delayed their onset. In both studies, effects of COX-1 deletion were nearly as protective as deletion of COX-2. As in our work, Tiano *et al.* (21) found that epidermal PGE_2 content was reduced in COX-1$^{-/-}$ animals, proliferation was little different from WT animals, and the frequency of apoptotic cells was increased.

Rodent chemical carcinogenesis models or genetic susceptibility approaches are often used for understanding how a particular treatment will have an impact on cancer (20, 29, 30). In this study, results using a relatively cumbersome photocarcinogenesis protocol indicated that selective COX-1$^{-/-}$ deletion is not helpful, despite strongly positive evidence of protection in other model systems (20, 21). This difference may be because of testing the effects of COX-1$^{-/-}$ deletion in the SKH strain rather than the NMRI strain typically used for chemical carcinogenesis, because strain differences in tumor susceptibility are common. Interestingly, some work has been done using NMRI mice to examine tumor development in response to UV irradiation compared with DMBA chemical carcinogenesis (31). This study demonstrated that irradiation produced tumors and papillomas in NMRI mice, although there were 30% more growths in the DMBA-treated animals. Given this comparison, it is important to consider that the lack of protection against UV photocarcinogenesis in SKH animals with COX-1$^{-/-}$ deletion may be because of how cancer is induced or promoted in these models. Nearly all of the skin cancers are caused by repeated exposure to sunlight (1, 3, 32), and extensive endogenous systems are present to repair the effects of this chronic environmental insult (2). In contrast, typical chemical carcinogenesis models have only a single initiation treatment when DMBA is applied, followed by repeated promotion without additional initiation (16).

Nonmelanoma skin cancer is extremely common. Each year, nearly a million Americans are diagnosed with a nonmelanoma skin cancer. The cost of treating these tumors is approximately $500 million annually. It is clear that effective skin cancer chemoprevention, reducing the need for surgical intervention, would be broadly beneficial (3, 4). A causal relationship between induced COX-2 expression and UV-induced development of skin cancer has been demonstrated in hairless SKH-1 mice (15, 18). In both of these studies, selective COX-2 inhibition suppressed tumor formation in response to chronic UV exposure. The clear implication is that selective COX-2 inhibition may be a useful intervention for populations at risk for nonmelanoma skin cancer. Such an intervention would likely be very broad-based, making it very important to be certain of the associated risks and benefits (13). Until the current study, research suggests that selective COX-1 inhibition would be helpful (20, 21). However, a model system, which uses UV light as the carcinogen revealed that this is not the case.

Several useful conclusions can be drawn from these studies. First, apoptosis is not a key method for decreasing tumor initiation or progression in photocarcinogenesis. Despite a 4-fold induction of

Table 3 *Average tumor size remains unchanged in COX-1$^{-/-}$ animals after chronic UV-induced skin irradiation*

	WT	COX-1$^{+/-}$	COX-1$^{-/-}$
Average tumor size (mm)	9.75 ± 1.32	9.1 ± 2.33	8.55 ± 1.13

NOTE: Comparison of tumor size after 15 weeks of UV irradiation revealed no significant differences between the genotypes. Data are expressed as the average size of tumors per mouse. Wild-type, $n = 8$; COX-1$^{+/-}$, $n = 10$; and COX-1$^{-/-}$, $n = 9$.

apoptosis in COX-1$^{-/-}$ animals, no substantive protection against skin cancer was evident. Second, and more important than the implication of these findings for skin cancer, are the more generalizable conclusions that can be drawn. In previous work, the efficacy of a cancer treatment or prevention strategy is usually linked with its capacity to enhance apoptosis (33–36). The ability to separate induction of apoptosis from protection against tumorigenesis is clearly demonstrated here, suggesting that although increased apoptosis may be helpful, it is not sufficient to provide cancer prevention. These results also confirm that tumorigenesis is specifically linked to the carcinogenic stimulus. Although ample evidence supports the unique mutational profile of various carcinogenic exposures, studies to develop treatments or chemoprevention strategies are often tested in models that may not replicate the etiology of the human cancer of interest. Because substantial resources must be invested in human chemoprevention studies, the work presented here indicates that models to test chemoprevention strategies must specifically consider cancer etiology in their design.

ACKNOWLEDGMENTS

We thank Carol Pearce for help with manuscript preparation.

REFERENCES

1. Ananthaswamy HN. Ultraviolet light as a carcinogen. In: Bowden GT, Fischer SM, editors. Comprehensive toxicology. New York: Elsevier; 1997. p. 253–70.
2. DeGruij F, van Kranen HJ, Mullenders LHF. UV-induced DNA damage, mutations and oncogenic pathways in skin cancer. J Photochem Photobiol B 2001;63:19–27.
3. Bruce A, Brodland DG. Overview of skin cancer detection and prevention for the primary care physician. Mayo Clin Proc 2000;75:491–500.
4. Strayer SM, Reynolds PL. Diagnosing skin malignancy: assessment of predictive clinical criteria and risk factors. J Fam Pract 2003;52:210–8.
5. Pentland AP. Arachidonic acid metabolism. In: Fitzpatrick's dermatology in general medicine. 5th ed. New York: McGraw-Hill; 1998.
6. Furstenberger G, Marks F. The role of eicosanoids in normal, hyperplastic and neoplastic skin. In: Ruzicka T, editor. Eicosanoids in the skin. Boca Raton, FL: CRC Press; 1990. p. 107–24.
7. Pentland AP, Mahoney M, Jacobs SC, Holtzman MJ. Enhanced prostaglandin synthesis after ultraviolet injury is mediated by endogenous histamine stimulation. J Clin Investig 1990;86:566–74.
8. Konger R, Malaviya R, Pentland AP. Growth regulation of primary human keratinocytes by prostaglandin E receptor EP2 and EP3 subtypes. Biochim Biophys Acta 1998;1401:221–34.
9. Smith WL, Garavito RM, DeWitt DL. Prostaglandin endoperoxide H synthase (cyclooxygenases-1 and -2). J Biol Chem 1996;271:33157–60.
10. Athar M, An KP, Morel KD, et al. Ultraviolet B (UVB)-induced COX-2 expression in murine skin: an immunohistochemical study. Biochem Biophys Res Comm 2001; 280:1042–7.
11. Buckman SY, Gresham A, Hale P, et al. COX-2 expression is induced by UVB exposure in human skin: implications for the development of skin cancer. Carcinogenesis 1998;19:723–9.
12. Chen W, Tang Q, Gonzolews MS, Bowden GT. Role of p38 MAP kinases and ERK in mediating ultraviolet-B induced cyclooxygenase-2 gene expression in human keratinocytes. Oncogene 2001;20:3921–6.
13. Church RD, Fleshman JW, McLeod HL. Cyclooxygenase 2 inhibition in colorectal cancer therapy. Br J Surg 2003;90:1055–67.
14. Pruthi RS, Derksen E, Gaston K. Cyclooxygenase-2 as a potential target in the prevention and treatment of genitourinary tumors: A review. J Urol 2003;169:2352–9.
15. Fischer SM, Lo H, Gordon GB, et al. Chemoprotective activity of Celecoxib, a specific cyclooxegenase-2 inhibitor, and indomethacin against ultraviolet light-induced skin carcinogenesis. Mol Carcinog 1999;25:231–40.
16. Marks F, Furstenberger G. Cancer chemoprevention through interruption of multistage carcinogenesis: lessons learnt by comparing mouse skin carcinogenesis and human large bowel cancer. Eur J Cancer 2000;36:314–29.
17. Marks F, Muller-Decker K, Furstenberger G. A casual relationship between unscheduled eicosanoid signaling and tumor development: cancer chemoprevention by inhibitors of arachidonic acid metabolism. Toxicology 2000;153:11–26.
18. Pentland AP, Schoggins JW, Scott GA, Khan KNM, Han R. Reduction of UV-induced skin tumors in hairless mice by selective COX-2 inhibition. Carcinogenesis 1999;20:1939–44.
19. Muller-Decker K, Kopp-Schneider A, Marks F, Seibert K, Furstenberger G. Localization of prostaglandin H synthase isozymes in murine epidermal tumors: suppression of skin tumor promotion by inhibition of prostaglandin H synthase-2. Mol Carcinog 1998;23:36–44.
20. Chulada PC, Morrow TB, Mahler JF, et al. Genetic disruption of Ptgs-1, as well as of Ptgs-2, reduces intestinal tumorigenesis in Min mice. Cancer Res 2000;60:4705–8.
21. Tiano HF, Loftin CD, Akunda J, et al. Deficiency of either cyclooxygenase (COX)-1 or COX-2 alters epidermal differentiation and reduces mouse tumorigenesis. Cancer Res 2002;62:3395–401.
22. Tripp CS, Blomme EAG, Hardy MM, LaCelle P, Pentland AP. Epidermal COX-2 induction after ultraviolet irradiation: Suggested mechanism for the role of COX-2 inhibition in photoprotection. J Investig Dermatol 2003;121:853–61.
23. Langenbach R, Morham SG, Tiano H, et al. Prostaglandin synthase 1 gene disruption in mice reduces arachidonic acid-induced inflammation and indomethacin-induced gastric ulceration. Cell 1995;83:483–92.
24. DeGruijl F, Forbes PD. UV-induced skin cancer in a hairless mouse model. Bioessays 1995;17:651–60.
25. Djabali K, Christiano AM. Hairless is a nuclear matrix associated protein with a putative chromatin remodeling function. J Investig Dermatol 2002;7:1330.
26. Panteleyev AA, Paus R, Ahmad H, Sundberg JP, Christiano AM. Molecular and functional aspects of the hairless (hr) gene in laboratory rodents and humans. Exp Dermatol 1998;7:249–67.
27. Brouxhon SM, Prasad AV, Joseph SA, Felten DL. Localization of corticotropin-releasing factor in primary and secondary lymphoid organs of the rat. Brain Behav Immun 1998;12:107–22.
28. Bradley J, editor. Distribution-free statistical tests. Englewood Cliffs, NJ: Prentice-Hall; 1968.
29. Neufang G, Furstenberger G, Heidt M, Marks F, Muller-Decker K. Abnormal differentiation of epidermis in transgenic mice constitutively expressing cyclooxygenase-2 in skin. Proc Natl Acad Sci USA 2001;98:7629–34.
30. Bol DK, Rowley RB, Ho CP, et al. Cyclooxygenase-2 overexpression in the skin of transgenic mice results in suppression of tumor development. Cancer Res 2001;62: 2516–21.
31. Makinen M, Stenback F. Skin tumor development and keratin expression in different experimental models. Relation to inducing agent and target tissue structure. Exp Toxicol Pathol 1998;50:199–208.
32. Dumaz N, van Kranen, HJ, de Vries A, et al. The role of UVB light in skin carcinogenesis through the analysis of p53 mutations in squamous cell carcinomas of hairless mice. Carcinogenesis 1997;15:897–904.
33. Ravi R, Bedi A. Potential methods to circumvent blocks in apoptosis in lymphomas. Curr Opin Oncol 2002;14:490–503.
34. Thornalley PJ. Isothiocyanates: mechanism of cancer chemopreventive action. Anti-Cancer Drugs 2002;13:331–8.
35. Kim R, Tanabe K, Emi M, et al. Inducing cancer cell death by targeting transcription factors. Anti-Cancer Drugs 2003;14:3–11.
36. Chetty R. p27 protein and cancers of the gastrointestinal tract and liver: an overview. J Clin Gastroenterol 2003;37:23–7.